 doi:10.20944/preprints202208.0158.v1

Article

Regulation Microglia Activation Mediated Neuroinflammation to Ameliorate Ischemia-reperfusion Injury via STAT5-NF-κB Pathway in Ischemic Stroke

Zhijun Pu [1,2,3,4,5], Shengnan Xia [1,2,3,4,5], Pengfei Shao [1,2,3,4,5], Xinyu Bao [1,2,3,4,5], Dan Wu[1,2,3,4,5] and Yun Xu [1,2,3,4,5*]

[1] Department of Neurology, Nanjing Drum Tower Hospital, The Affiliated Hospital of Medical School of Nanjing University, Nanjing, Jiangsu 210008, P.R. China
[2] Institute of Brain Sciences, Nanjing University, Nanjing, Jiangsu 210093, P.R. China
[3] Jiangsu Key Laboratory for Molecular Medicine, Medical School of Nanjing University, Nanjing, Jiangsu 210008, P.R. China
[4] Jiangsu Province *Stroke* Center for Diagnosis and Therapy, Nanjing, Jiangsu 210008, P.R. China
[5] Nanjing Neurology Clinic Medical Center, Nanjing, Jiangsu 210008, P.R. China
*Corresponding author: xuyun20042001@aliyun.com

Abstract: Inflammatory reaction after ischemia-reperfusion contributes significantly to prognosis, and microglia activation is the main resource of inflammation in nervous system. STAT5 is proving to be a highly effective anti-inflammatory therapy with great potential, and inhibition of STAT5 has demonstrated significant anti-inflammation and therapeutic effects, but rarely focus on mechanism of neuroinflammation and brain injury from ischemia-reperfusion. It is the first time to found that the anti-inflammation of dauricine is mainly through STAT5-NF-κB pathway, might act as a STAT5 inhibitor. Dauricine suppressed the inflammation cytokines Eotaxin, KC, TNF-α, IL-1α, IL-1β, IL-6, IL-12β, IL-17α, and also inhibited the microglia activation. STAT5b mutant at Tyr-699 reversed the protective effect of dauricine on oxygen-glucose deprivation-reperfusion injury of neurons, and re-activated the suppression of dauricine on P-NF-κB of microglia. These results suggest that dauricine might suppress the neuroinflammation and protect the neuron from the injury of post-ischemia-reperfusion via mediating the microglia activation through STAT5-NF-κB pathway, and ss a potential therapeutic target for neuroinflammation, STAT5 needs to be raised concern in ischemic stroke.

Keywords: dauricine; STAT5; NF-κB; Inflammation; Ischemia-reperfusion injury

1. Introduction

Inflammation is closely related to both injury and repair processes after stroke, and has been supported to be a causal role in pathogenesis of stroke(Kelly et al., 2021). Inflammation that persists is linked to a bad prognosis, and a higher baseline level of inflammation predicts short-term poor outcomes in large stroke(Hou et al., 2021). Microglia is the only resident immunoreactive cells in the brain, plays an important role as the first line of defense against central nervous system injury and inflammation, and can be activated within minutes of ischemic brain injury(Goshi et al., 2020; Ma et al., 2017). The identification of early recurrent stroke was improved by the symptomatic carotid atheroma inflammation lumen-stenosis score(Kelly et al., 2020), and plaque inflammation-related f-fluorodeoxyglucose uptake independently predicted future recurrent stroke post-PET(Kelly et al., 2019). The clinical outcomes after acute ischemic stroke could be improved by targeting the immunity and inflammation(Zhang et al., 2018).

Dauricine ($C_{38}H_{44}N_2O_6$) is a monomer of Chinese traditional herbs with rich p harmacological activity, especially in anti-inflammation and neuroprotection. By in hibiting the NF-κB pathway, dauricine may be able to reduce endothelial inflamm ation(Hu et al., 2021), inhibits the inflammatory response generated by LPS or cec al ligation and puncture(Qiao et al., 2019), and inhibits severe pneumonia co-infect

 doi:10.20944/preprints202208.0158.v1

ed with streptococcus pneumoniae combining with clindamycin(Li et al., 2018). Da uricne plays a neuroprotective role mainly through upregulating GPX4 expression to inhibit ferroptosis of nerve cells after intracerebral hemorrhage(Peng et al., 2022), inhibiting inflammatory process after focal cerebral ischemia/reperfusion(Yang et al., 2007), and inhibiting HERG encoded potassium channels(Zhao et al., 2012). It i s certain the anti-inflammation that dauricine plays, however, the anti-inflammatio n target of dauricine remains unknown.

In this study, we found a new anti-inflammation mechanism of dauricine that is STAT5-NF-κB pathway, might acted as a STAT5 inhibitor, dauricine not only reduced the inflammation reaction induced by LPS or injury of ischemia reperfusion through regulating the microglia activation, but also rescued the neurons from injury of post-ischemia-reperfusion in ischemia stroke mouse model.

2. Materials and methods

2.1. Cell culture and treatment

As described previously(Meng et al., 2019), mice 24-hours-old C57BL/6J were used to isolate and purify primary microglial cells. The cortical neurons were isolated from C57BL/6J mice embryos at the E15-17 stage(Zhang et al., 2020). Here won't describe in detail. The microglial cells were acquired and replaced onto the indicated plates with new complete medium, and primary neurons were cultured in medium containing B27 (Life Technologies, B27 supplement 50×, 17504) and glutamine (Gibco, GlutaMAX™ 200Mm (100×), 35050061).

Dauricine was purchased from MUST (ChengDu, China, A0315), dissolved in DMSO for mother liquor, and diluted with medium when treating cells. Limitation of drug administration capacity in mice studies(Li and Gong, 2007) (Yang et al., 2010), dauricine finally presented as a turbid liquid in 0.9% NaCl saline. There are many studies of dauricine about transient focal cerebral ischaemia in rat and mouse, and the neuroprotective dose is from 5 to 10 mg/kg, so we chose the dosage of 10 mg/kg in this study(Yang et al., 2010). The dosage was 10 mg/kg and the volume of administration was 10 mL/kg for intragastric administration. One dose at the first reperfusion of fecal cerebral ischemia within 30 mins, one dose per day. An experiment was conducted on primary microglia cells, in which dauricine or vehicle were pre-treated for 1h, followed by LPS (200ng/mL) to stimulate inflammation, and collected the cell samples for next detection.

2.2. Oxygen-glucose deprivation-reperfusion

Oxygen-glucose-deprivation-reperfusion (OGD-R) models of primary cortical neurons are a well-accepted model of cerebral ischaemia reperfusion in vitro(Guo et al., 2018). Briefly, the culture mediums for neurons were substituted with Neurobasal™-A medium (1×) liquid that contained no glucose, and the gas mixture composed of 95% N_2 and 5% CO_2 was substituted for the gas with 5% CO_2 for 15 mins through a hypoxia chamber (Billups-Rothenberg, USA). Chamber was sealed and incubated at 37 °C for 15 mins, then culture mediums were substituted to normal medium with glucose and dauricine or DMSO, and incubated in 37 °C with 5% CO_2 for 3 h.

2.3. Cell viability assays

The viability of neurons was detected by the CCK-8 (Dojindo Laboratories, CK04) and cytotoxicity detection kit (LDH) (Roche, 11644793001). Post-treatment of OGD and drug for 1h, then underwent OGD-R for 3h, next 50 μL cell supernatant was taken each well of 96-well plates and added 50 μL LDH working mixture away from light, and the cell was added new medium with CCK-8 at 37 °C for 1-4 h. Respectively, the absorbance at 450 nm (CCK-8) and 490 nm (LDH) was measured by a microplate reader. The result of cell viability was presented as the percentage of living cells to control cells.

 doi:10.20944/preprints202208.0158.v1

2.4. Calcein acetoxymethylester/propidium iodide AM/PI staining assay

Calcein - AM/PI Double Stain Kit (Dojindo Laboratories, C542) was used to detect the viability of neurons. Primary cortical neuron was treated with OGD-R, and then incubated with the calcein-AM and PI buffer in 37 °C with 5% CO_2 for 15 mins away from light, next captured with a fluorescence microscope (OLYMPUS, IX73P1F). The viable cells with green fluorescence, and dying cells with red fluorescence, so the viability of neurons was counted with the ratio of green fluorescence to green fluorescence and red fluorescence.

2.5. Middle cerebral artery occlusion in mice

The experimental animal ethics review protocol for Drum Tower Hospital at Nanjing University has been approved, the Experimental Animal Ethics Committee has examined the protocol**,** and the studies were conducted according to the guidelines set by Nanjing University's Guide for Animal Care and Use Committee. All mice experiments were conducted with C57BL/6J (B6) mice (eight weeks old; 20 to 24 g body weight) obtained from Nanjing University's Animal Model Centre. Under anesthetizing with isoflurane, the middle cerebral artery was blocked with 6-0 surgical monofilament nylon sutures (Doccol Corporation, USA), and caused the decrease of the blood flow to below 20%(Egashira et al., 2013; Zhang et al., 2020). The blood flow was restored in the middle cerebral artery (MCA) region followed occlusion for 1h. In the sham control mice, the same operation was applied instead of insertion of the 6-0 surgical monofilament nylon sutures into the MCA. We have a mature and stable technical team, the mortality is controlled about at 20%, and the success rate of model is controlled up to 80%.

2.6. Infarct volume calculation

The mice were euthanized at day 7 after focal cerebral ischemia, and the infarct volume of brain tissue was measured. After cutting the brains coronally into six seria1 1-mm slices, then immersed in 2% TTC (2,3,5-triphenyltetrazolium chloride, Sigma, T8877) for 20 mins(Wu et al., 2019). ImageJ (the National Institutes of Health, version 1.8.0_172) was used to analyze the images with TTC, and the infarct volume is expressed with the formula for calculating : Percentage lesion volume (%) = (left hemisphere volume - right uninfarcted volume) / (left hemisphere volume × 2) × 100% (Cen et al., 2013).

2.7. Neurological deficit scoring

Neurological function of mice was evaluated until day 7 after MCAO(Meng et al., 2021), including rotarod test, forelimb grip strength test, and the modified neurological severity score (mNSS) test. Grip strength meter (BIOSEB, USA) was used to measure the forelimb grip strength. In triplicate, the strength of the grip was recorded before release, and the average was recorded at the previous day, day 1, 3 and 7 after MCAO(Alamri et al., 2018). The Rotarod Test (IITC Life Science, USA) was applied to assess motor deficits and sensorimotor coordination, and measurements were taken on the previous day, on day 1, 3 and 7 after MCAO(Zhang et al., 2011). The mNSS test measures sensory function, motor function, reflexes, and balance, and was administered on day 1, 3 and 7 after MCAO(Chen et al., 2001). During the rating of mice, the investigator was blinded to the experimental groups.

2.8. Cerebral blood flow measure

Utilizing the PeriFlux System 5000 (Perimed AB, Sweden), the cerebral blood flow is strictly monitored during MCAO modeling, and verification of model success and injure was measured the cerebral flood flow by PeriCam PSI (Perimed AB, Sweden) at post-operation.

Preprints (www.preprints.org) | NOT PEER-REVIEWED | Posted: 8 August 2022 doi:10.20944/preprints202208.0158.v1

2.9. RNA isolation and quantitative real-time PCR

Tissue and cell samples were lysed and extracted with RNA Isolation Kit (FastPure Cell/Tissue Total RNA Isolation Kit V2, Vazyme, RC112). Quantitative real-time PCR was performed in a Roche LightCycler ® 96 system (Roche, Germany) with a SYBR green kit (Accurate, China, AG11701). The primers are as follows:

TNF-α: forward primer- CCTGTAGCCCACGTCGTAG; reverse primer- GGGAG-TAGACAAGGTACAACCC;

IL-1β: forward primer- GAAATGCCACCTTTTGACAGTG; reverse primer-TGGATGCTCTCATCAGGACAG;

IL-6: forward primer- TAGTCCTTCCTACCCCAATTTCC; reverse primer-TTGGTCCTTAGCCACTCCTTC;

GAPDH: forward primer- AGGTCGGTGTGAACGGATTTG, reverse primer-TGTAGACCATGTAGTTGAGGTCA;

β-Actin: forward primer- GGCTGTATTCCCCTCCATCG, reverse primer- CCAGTT-GGTAACAATGCCATGT.

2.10. RNA Sequence

The sequence was performed by Majorbio (Shanghai, China), based on Illumina Novaseq 6000 Sequencing platform. The percentage of Q30 base was above 95.73%, and the clean data of each sample was above 6.35 Gb. Based on the quantitative results of expression levels, the differential genes between groups were analyzed, including differential Venn analysis, Reactome enrichment analysis, functional enrichment analysis, cluster analysis, and KEGG enrichment analysis.

2.11. Cytokine analyses in cellular supernatant

Wayen Biotechnologies (Shanghai, China) performed the Luminex liquid suspension chip, and monitored the concentration of cytokine in cellular supernatant with the Bio-Plex Mouse Panel 23-plex Cytokine kit(Wei et al., 2021). In brief, 50 μL samples or standard substance were added into 96-well plates, and incubated for 30 mins in room temperature and away from light, then added 25 μL diluted detection antibody and incubated for 30 mins as before, next added 50 μL diluted streptavidin-PE and incubated for 10 mins. Finally, the signal was measured by Bio-Plex 200 System (Luminex Corporation, Austin, TX, USA).

2.12. Western blot assay

RIPA lysis buffer (Thermo Scientific, USA, 89901) was used to extract the total proteins. In brief, 10% SDS-PAGE was adopt to separate the protein and the protein was electrophoretically transferred onto 0.2 μm PVDF membranes (Immobilon-PSQ Transfer membrane, Merck Millipore, ISEQ00010), and 5% skim milk were applied to block the membranes for 2 h at room temperature, then incubated at 4°C as least 12 h with the antibodies: anti-Stat5 antibody (CST, 9363S, 1:1000), anti-phospho-Stat5 antibody (CST, 4322S, 1:1000) (endogenous levels of Stat5a only when phosphorylated at Tyr694 and Stat5b when phosphorylated atTyr699), anti-P-NF-kB antibody (CST, 3033S, 1:1000), anti-NF-κB antibody (CST, 8242S, 1:1000), anti-β-tubulin antibody (Bioworld Technology, AP0064, 1:2000), anti-β-actin antibody (Bioworld Technology, AP0060, 1:2000). Corresponding secondary antibodies were chosen to combine the membranes for 1 hour at room temperature and were visualized with the Chemiluminescent HRP Substrate (Millipore, USA, WBKLS0500), ImageJ (the National Institutes of Health, version 1.8.0_172) was used to quantify the bands with gray value. The relative protein expression was expressed with the band intensity to the β-tubulin.

Preprints (www.preprints.org) | NOT PEER-REVIEWED | Posted: 8 August 2022 doi:10.20944/preprints202208.0158.v1

2.13. Immunofluorescence staining in brain sections and microglia cells

Mice, under deep anesthetized, were perfused with PBS and 4% paraformaldehyde through left ventricle, followed dehydrated with glucose solution, and sectioned with 20 μm thickness. Primary microglia cell was treated with lipopolysaccharide or dauricine for 3 h, then discarded the supernatant and fixed in 4% paraformaldehyde for 15 mins, 0.25% Triton X-100 was used to permeabilize for 15 mins, then 2% bovine serum albumin was applied to block for 2 h, followed by incubating with indicated anti-Iba1 antibody (Abcam, ab5076, 1:100) at 4°C for at least 12 h. Next day, antibody was recycled and cells was gently washed 3 times by PBS, and then corresponding secondary antibodies with 594 nm wavelength (Invitrogen, 1:500) was incubated for 2 h, avoiding light, at room temperature. DAPI staining kit (Bio-world, BD5010, 1:1000) was used to counterstain the nuclei. Fluorescence microscope (OLYMPUS, IX73P1F) and confocal laser scanning microscope (OLYMPUS, FV3000) were applied to obtain the images, and positive amount was quantified with ImageJ (the National Institutes of Health, version 1.8.0_172).

2.14. Ligand–receptor docking and analysis

AutoDock 4 program (version 4.2.6) was adopted to perform the Ligand–receptor docking. The binding site was analyzed, and images were generated with PyMOL, version 2.2.0(Seeliger and de Groot, 2010). The STAT5a and STAT5b 3D protein structure are from PDB (Protein Data Bank, www.rcsb.org). The dauricine 3D structure is from PubChem (pubchem.ncbi.nlm.nih.gov).

2.15. Plasmid construction and transfection

We acquired the STAT5b transcription (NM_001113563) from NCBI (https://www.ncbi.nlm.nih.gov), and designed the STAT5b overexpression vector (pLV11ltr-Puro-mCherry-CMV-STAT5b) (Abbr: STAT5b OV) and STAT5b mutant at Tyr-699 (pLV11ltr-Puro-mCherry-CMV-STAT5b(Y699A)) (Abbr: STAT5b (Y699A)). By point mutation primer, PCR point mutation was performed to mutate the 699th amino acid Tyr (Tyrosine) to Ala (Alanine). The plasmid construction work was mainly done by Nanjing Corues Biological Co., LTD, after sequencing reaction, the target sequence was verified to be correctly connected to the target vector. Plasmid transfection is performed according to the instruction of Lipofectamine™ 3000 (Invitrogen, L3000015), 48h later, the expression of red fluorescence (mCherry) was observed under fluorescence microscope, and the fluorescence expression rate directly reflected the cell transfection rate.

2.16. Statistical analysis

All values are expressed with the mean ± SEM, and unpaired Student's t test was used for two-group comparisons and two-way ANOVA followed by Dunnett's test for multiple pairwise comparisons was used to analyze the quantitative variables. Statistically significant was defined with $P<0.05$. GraphPad Prism 8 (GraphPad Software, USA, version 8.0.2) was performed the statistical graph.

3. Results

3.1. Dauricine decreased neuron death induced by OGD-R

First, we examined the potential neurotoxicity of dauricine on primary neuron through adding different concentrations of dauricine to the media for 3h, then determined the LDH of culture supernatant and CCK8 of cells. The compound structure of dauricine is as presented in **Figure 1A**. Dauricine did not decrease the cell viability and showed no significantly cytotoxicity for primary neuron below 40 μM (**Figure 1B and 1C**), and the results of LDH and CCK8 were the same trend, so the cell viability of OGD-R-treated neurons was detected by LDH of cell supernatant, and found the significantly increased by dauricine (1 μM) ($P < 0.01$; **Figure 1F**). Furthermore, dauricine treatment partially rescued

Preprints (www.preprints.org) | NOT PEER-REVIEWED | Posted: 8 August 2022 doi:10.20944/preprints202208.0158.v1

the neuronal cell death induced by OGD-R, shown by calcein-AM and PI staining ($P < 0.05$; **Figure 1D and 1E**).

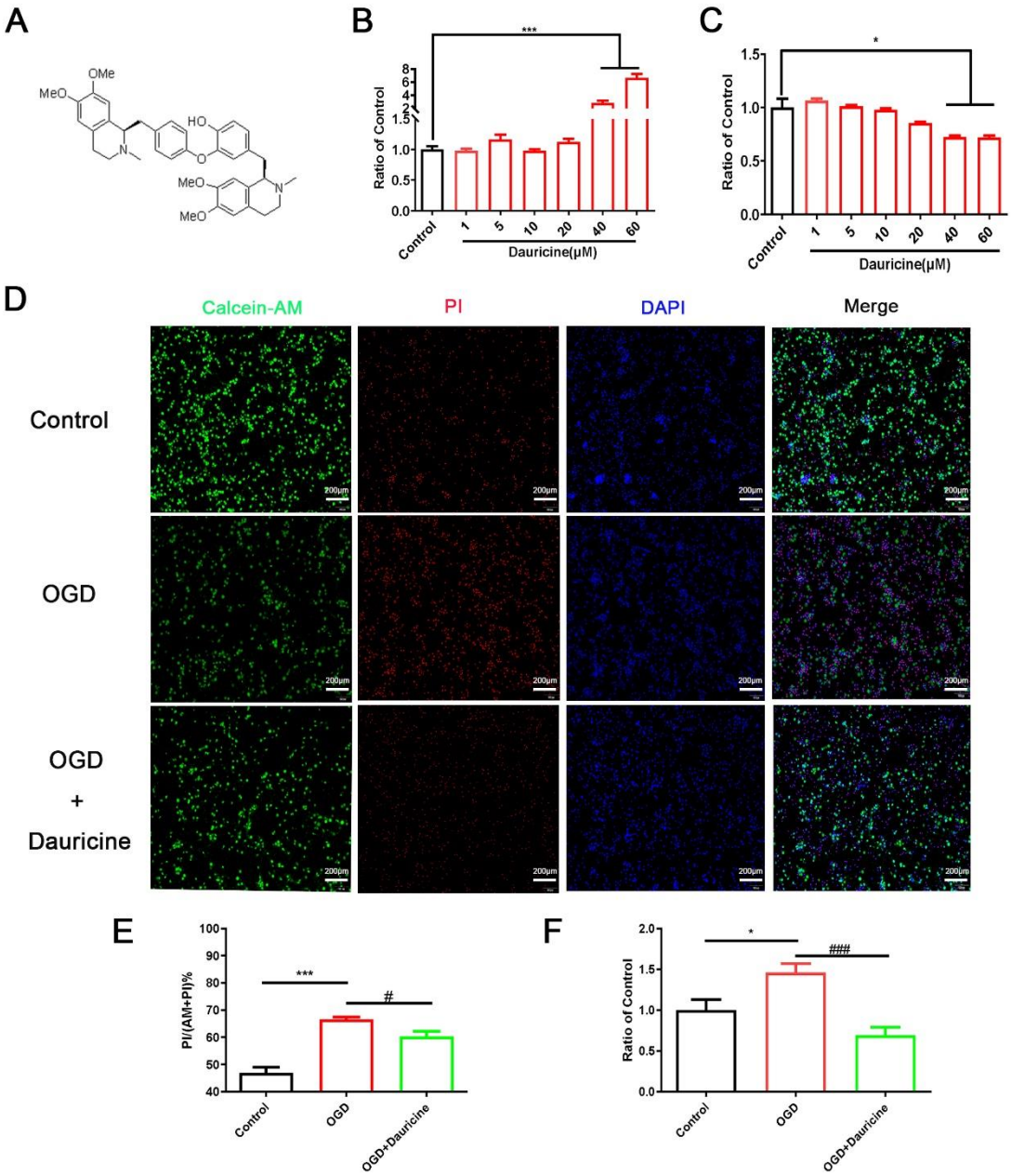

Figure 1. Dauricine decreased primary neuron death induced by OGD-R. (A) The compound structure of dauricine. (B) LDH of primary cortical neurons cell supernatant, and (C) CCK8 of primary cortical neurons cell were detected followed dauricine (1, 5, 10, 20, 40, 60 μM) treatment of 24h, n = 5. Control group vs Dauricne group, ***p < 0.001. Oxygen-glucose deprivation of primary cortical neurons cell for 15 mins, then reperfused and treated with dauricine (1 μM) for 3 h, (F) the viability of primary cortical neurons cell was detected by LDH, cell viability was also showed by calcein-AM and PI buffer(D), and quantified(E), n = 5. Control group vs OGD group, *p < 0.05, ***p < 0.001; OGD group vs (OGD + Dauricine) group #p < 0.05, ###p < 0.001, unpaired Student's t test.

3.2. Dauricine decreased brain infarct size and neurological deficits after tMCAO injury

We verified whether the administration of dauricine has the same neuroprotection as in vitro. An infarction of the right hemisphere was developed after 1 h of MCAO, followed by reperfusion after 1 day, 3 day and 7 day. The cerebral blood flow after MCAO has been seen that the blood flow of infarct side brain significantly dropped, and shown the success of model (**Figures 2A**). TTC staining was used to evaluate the cerebral infarct

Preprints (www.preprints.org) | NOT PEER-REVIEWED | Posted: 8 August 2022 doi:10.20944/preprints202208.0158.v1

volume, and compared to the vehicle-treated group, the administration of dauricine showed a 56% reduction in infarct volume at 7 day after MCAO (**Figure 2B-2C**; P <0.05). As shown in **Figures 2D-2F,** the group treated with dauricine had significantly better neurological function at day 3 and day 7 after MCAO than the vehicle-treated group (P <0.05).

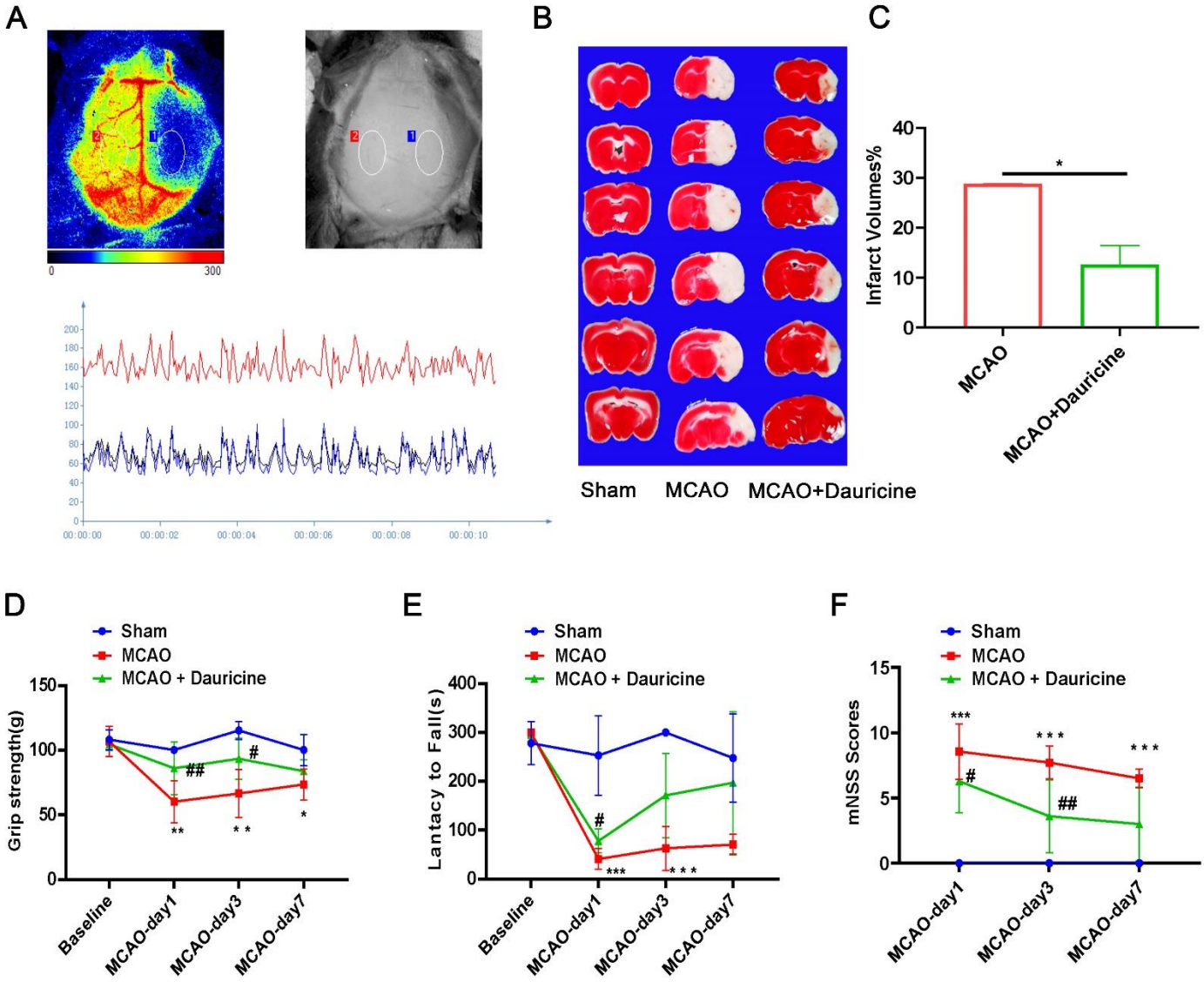

Figure 2. Dauricine improved the tMCAO injury. (A)The cerebral blood flow after MCAO, anatomy and infrared image are up, quantitative figure is below. (B) Mouse brains were procured at day 7 after ischemia reperfusion, and the infarct volume was determined by TTC staining, and quantified (C) (*p < 0.05). The functional outcomes of tMCAO mice were evaluated by (D) Grip strength, lantacy to fall (E), mNSS scores (F). n = 10 mice per group, Sham group vs MCAO group, **p < 0.01, ***p < 0.001; MCAO group vs (MCAO + Dauricine) group #p < 0.05, ##p < 0.01, two-way ANOVA with Bonferroni post hoc test.

3.3. Dauricine inhibited the activation of microglia in vitro and in vivo

Iba1 is a marker of microglia cell activation, and microglia displays as amebocyte when it is activated, so cell area also partly represents the activation of microglia cell. It was found that dauricne inhibited the activation of microglia from injury brain in three dimensional and plane (**Figure 3A**). Then the dauricine was also found to reduce the activation and cell area of amoeboid microglia cell induced by LPS in vitro (**Figure 3B-3D**).

Preprints (www.preprints.org) | NOT PEER-REVIEWED | Posted: 8 August 2022 doi:10.20944/preprints202208.0158.v1

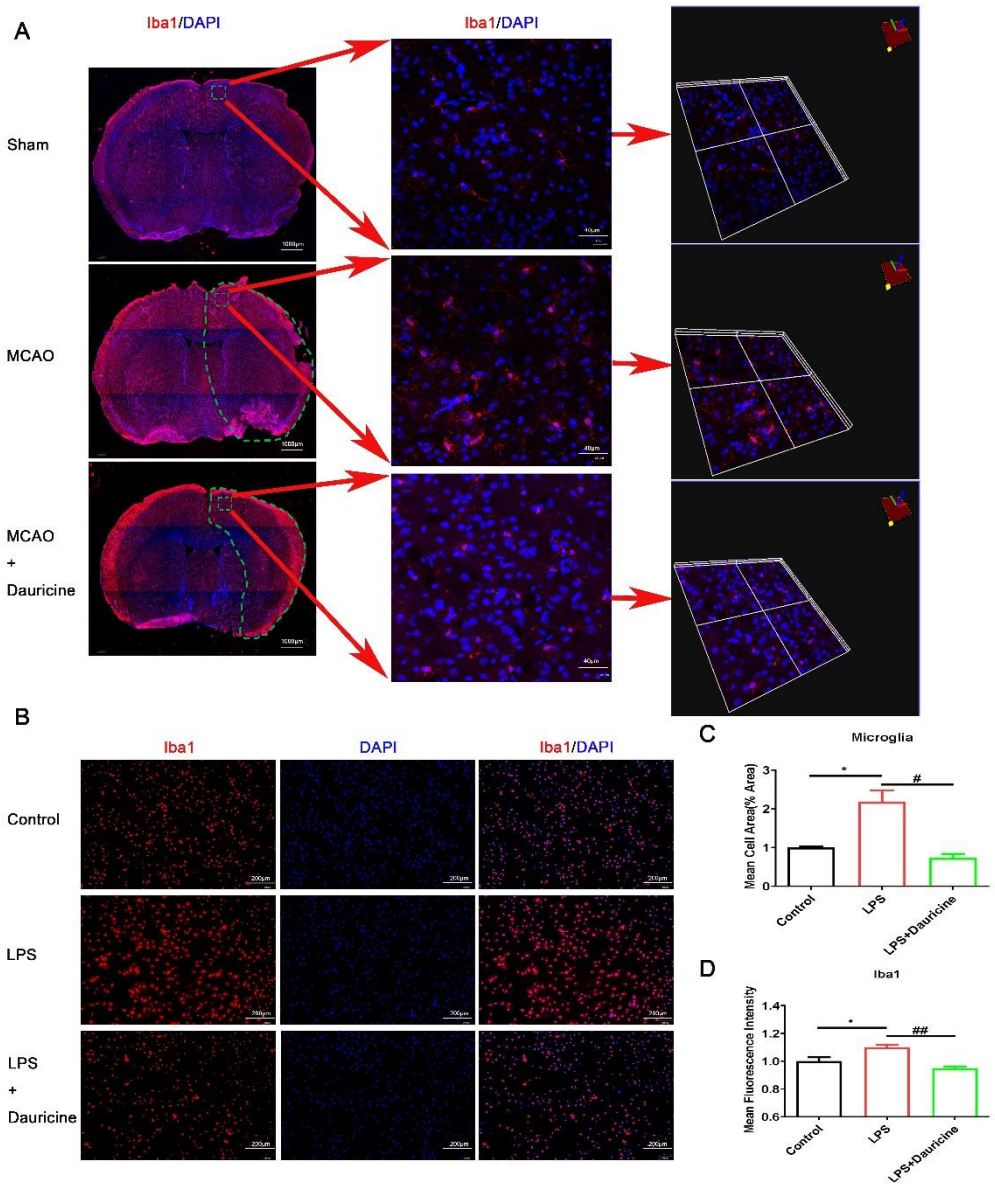

Figure 3. Dauricine inhibited the activation of microglia in vitro and in vivo. (A) The representative figures of brain sections in MCAO day 7, strained with immunofluorescence of Iba1 and DAPI were shown with full brain and three dimensional. (B) The representative figures of primary microglia cells induced by LPS or dauricine for 3 h in vitro, mean cell area (%) of microglia cell was counted (C), and mean fluorescence intensity of Ibal was counted (D). n = 3, Control group vs LPS group, *p < 0.05, **p < 0.01, ***p < 0.001; LPS group vs (LPS + Dauricine) group, #p < 0.05, ##p < 0.01, unpaired Student's t test.

3.4. Dauricine reduced inflammation induced by LPS or tMCAO injury

Inflammation is a causal role in the pathogenesis of stroke and is supported by diverse sources of evidence. The anti-inflammation of dauricine was investigated on the primary microglia induced by LPS. Primary microglia samples collected followed the dauricine (1 μM) pretreatment for 1 h and LPS or dauricine stimulation for another 3 h, then inflammation factors expression was detected by q-RT-PCR. We found that inflammation biomarkers IL-1β, IL-6 and TNF-α were significantly increased by LPS and reduced by dauricine in vitro **(Figures 4A-4C)**. The same tendency was got in the ischemic penumbra of tMCAO day 7, as shown in **Figures 4D-4G.**

Inflammation and immune cytokines communicate and work with cells mainly through proteins, so we measured the inflammation cytokines using Luminex liquid suspension chip for the cell supernatant. With the LPS- induced inflammation storm,

Preprints (www.preprints.org) | NOT PEER-REVIEWED | Posted: 8 August 2022 doi:10.20944/preprints202208.0158.v1

dauricine significantly reduced the cytokines as follow (**Figure 4H-4O**): Eotaxin, KC, TNF-α, IL-1α, IL-1β, IL-6, IL-12β, IL-17α.

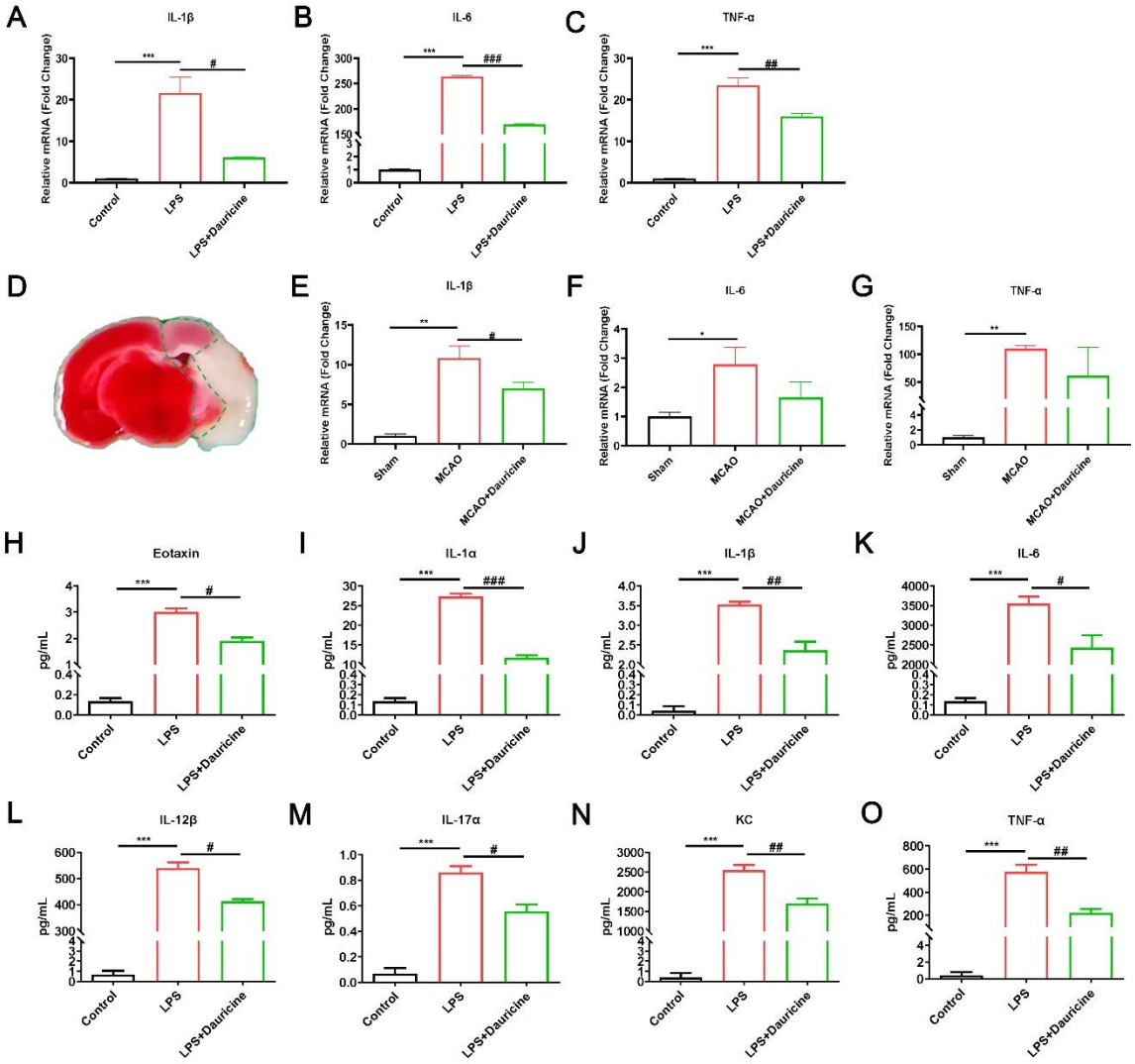

Figure 4. Dauricine decreased inflammation induced by LPS or tMCAO injury. LPS or dauricine stimulated primary microglia for 3 h, and inflammation mRNA IL-1β (A), IL-6 (B) and TNF-α (C) expressed, n = 3. Control group vs LPS group, ***p < 0.001; LPS group vs (LPS + Dauricine) group, #p < 0.05, ##p < 0.01, ###p < 0.001, unpaired Student's t test. Diagram of ischemic penumbra (D) and analysis of the inflammation mRNA IL-1β (E), IL-6 (F) and TNF-α (G) expressed at tMCAO day 7, n=3. The inflammation cytokines measured by Luminex liquid suspension chip for the cell supernatant, and cytokines as follow: Eotaxin (H), IL-1α (I), IL-1β (J), IL-6 (K), IL-12β (L), IL-17α (M), KC (N), TNF-α (O), n=3, Control group vs LPS group, ***p < 0.001; LPS group vs (LPS + Dauricine) group, #p < 0.05, ##p < 0.01, ###p < 0.001, unpaired Student's t test.

3.5. Dauricine down-regulated immune factors expression

RNA sequencing was applied to further explore the mechanism of dauricine reducing inflammation. The distribution of reads compared to the genome in different regions of the reference genome was statistically analyzed and the percent of reads mapped to genome regions was shown, and CDS made up 71.95% (**Figure 5A**). Compared with the LPS group, the dauricine group had 542 upregulated genes and 313 downregulated genes (pad-just ≤ 0.05, fold ≥ 1.5) (**Figure 5B**). Venn analysis shown that 188 genes were common contains among the gene sets control vs LPS and LPS vs LPS+Dauricine (**Figure 5C**). The reactome enrichment analysis revealed that the main reactome pathways were G alpha(q)

signaling events and cytokine signaling in immune system in LPS vs LPS+Dauricine (**Figure 5D**). Therefore, we focused on the common 188 genes and immune system down sets, and Venn analysis also confirmed that 14/15 genes of immune system down were included in the common 188 genes set (**Figure 5E**), then functional enrichment analysis refers to the enrichment analysis of the 14 gene sets, and the hypergeometric distribution algorithm is used to obtain the significant enrichment function of genes in the gene set (**Figure 5F**). The heatmap of immune system down set shown the 15 genes expression among control, LPS and LPS+Dauricine groups (**Figure 5G**). To further explore the pathway of immune system down, the KEGG enrichment analysis was applied and shown the JAK-STAT, TNF, and NF-κB signaling pathways involved (**Figure 5H**).

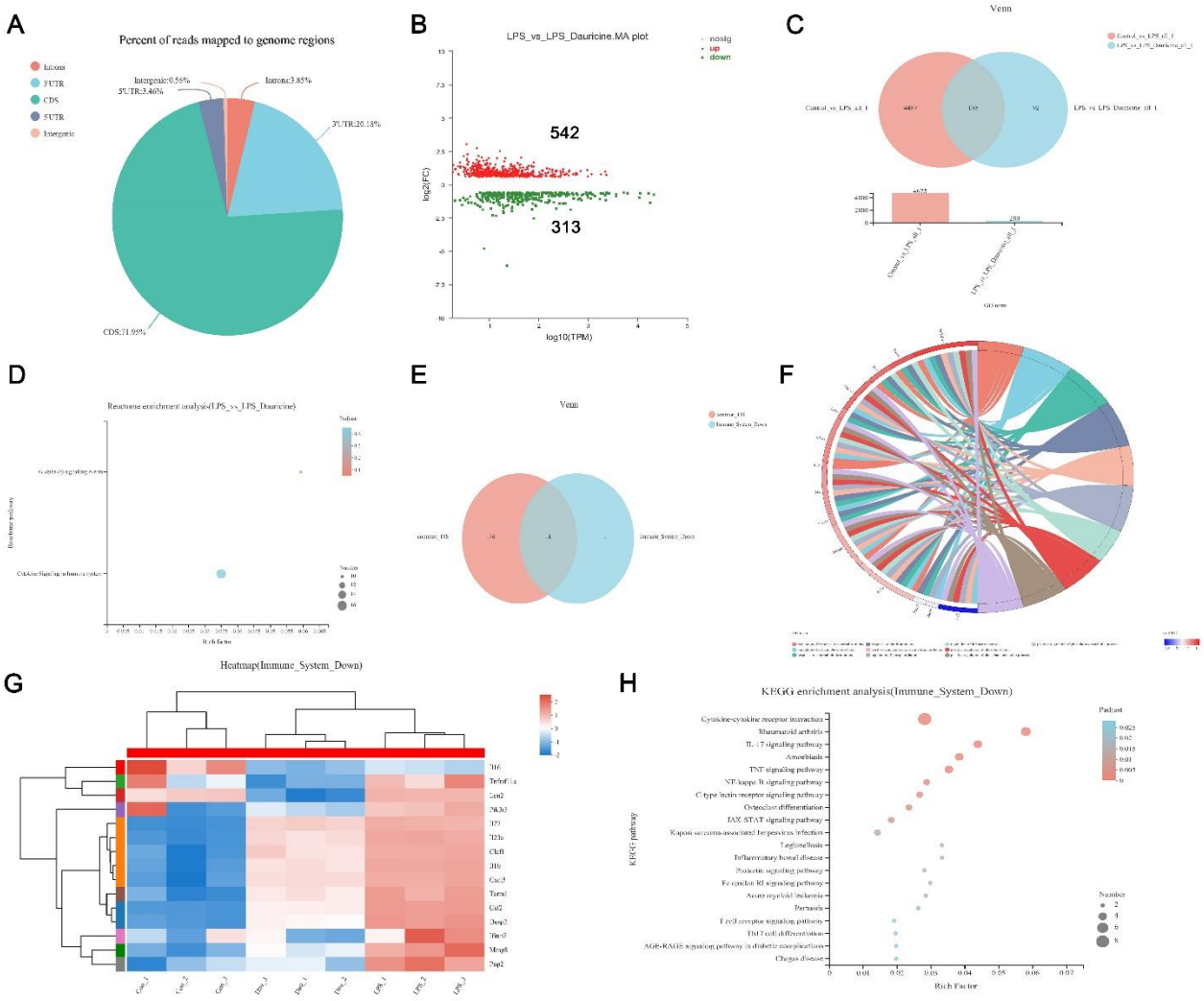

Figure 5. Transcriptomics of LPS or dauricine stimulated primary microglia. (A) Percent of reads mapped to genome regions. (B) MA diagram of expression difference between the LPS and LPS + dauricine groups. (C) Venn analysis between the Control vs LPS and LPS vs LPS + dauricine sets. (D) Reactome enrichment analysis of LPS vs LPS + dauricine set. (E) Venn analysis between the common 188 genes and immune system down sets. (F) Hypergeometric distribution algorithm to the enrichment analysis of the 14 gene sets from the common portion of the common 188 genes and immune system down sets. (G) Heatmap of the immune system down set, and KEGG enrichment analysis of the immune system down set (H).

3.6. Dauricine inhibited the activation of STAT5 and NF-κB pathways

JAK-STAT and NF-κB signaling pathways have been singled out by RNA sequencing, which might be involved in the inflammation regulated by dauricne. Therefore, we focused on the protein expression and modification of JAK-STAT and NF-κB signaling

Preprints (www.preprints.org) | NOT PEER-REVIEWED | Posted: 8 August 2022 doi:10.20944/preprints202208.0158.v1

pathways. We found that dauricine significantly inhibited the P-STAT5 and P-NF-κB induced by LPS in microglia cells (**Figure 6A-6C**), which indicated that dauricine reduced the inflammation might through regulating the STAT5-NF-κB signaling pathway.

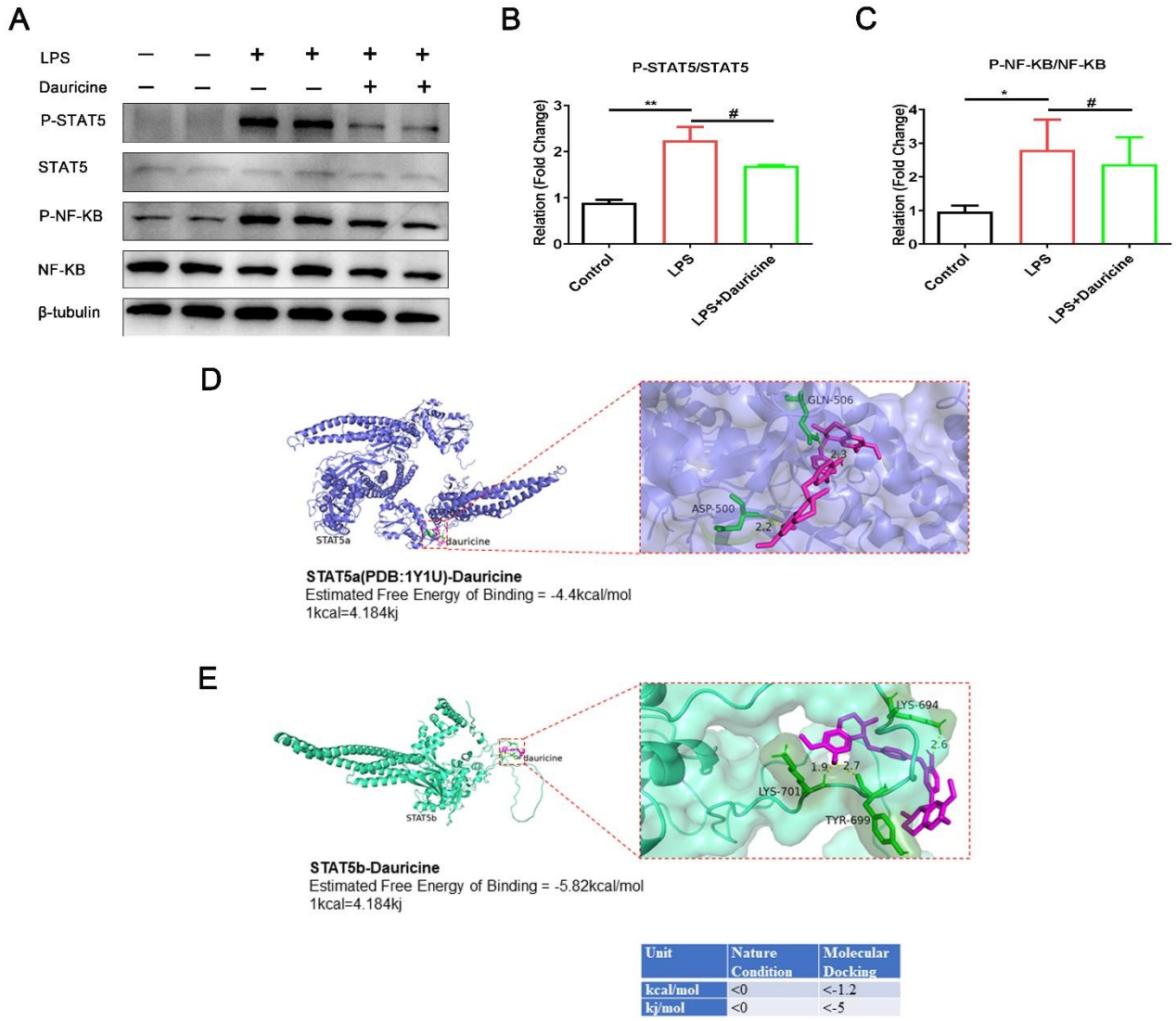

Unit	Nature Condition	Molecular Docking
kcal/mol	<0	<-1.2
kj/mol	<0	<-5

Figure 6. Dauricine inhibited the activation of STAT5, NF-κB and docked with STAT5. (A)The western blot representative figure of NF-κB, P-NF-κB, STAT5, P-STAT5 and β-tubulin were shown, and was counted with ratio of P-STAT5 to STAT5 (B) and P-NF-κB to NF-κB (C). n = 3, Control group vs LPS group, *p < 0.05, **p < 0.01, ***p < 0.001; LPS group vs (LPS + Dauricine) group, #p < 0.05, ##p < 0.01, unpaired Student's t test. Ligand receptor docking was performed with AutoDock and analyzed with PyMOL. The top panel shows the joint diagram of dauricine and STAT5a protein(D), and the lower panel shows the joint diagram of dauricine and STAT5b protein (E), the energy data under natural conditions and molecular docking is noted at bottom right.

Ligand–receptor docking was performed with AutoDock and analyzed with PyMOL. The molecular docking energy (< - 5 kj/mol) was low enough, which demonstrated that dauricine can directly bind with STAT5b at Tyr-699, the main phosphorylated region (**Figure 6E**), but the binding forece with STAT5a was not so well (**Figure 6D**). It was indicated that dauricine might target the STAT5b to make effects.

3.7. STAT5b (Tyr699 mutant) reversed the neuroprotection of neuron and activated the NF-κB pathway of microglia

Preprints (www.preprints.org) | NOT PEER-REVIEWED | Posted: 8 August 2022 doi:10.20944/preprints202208.0158.v1

To further clarify the neuroprotective and anti-inflammatory effects of dauricine by directly targeting STAT5 and inhibiting STAT5b phosphorylation, we constructed STAT5b overexpression plasmid (STAT5b OV) and STAT5b phosphorylation site Tyr-699 mutation-STAT5b (Y699A) plasmid (**Figure 7A-7B**) to intervene neurons, and the results showed that STAT5b (Y699A) reversed the protective effect of dauricine on oxygen-glucose deprivation-reperfusion injury of neurons (**Figure 7C-7D)**. The result suggested that dauricine might directly bind to Tyr-699 phosphorylation region of STAT5b to achieve its neuroprotective effect.

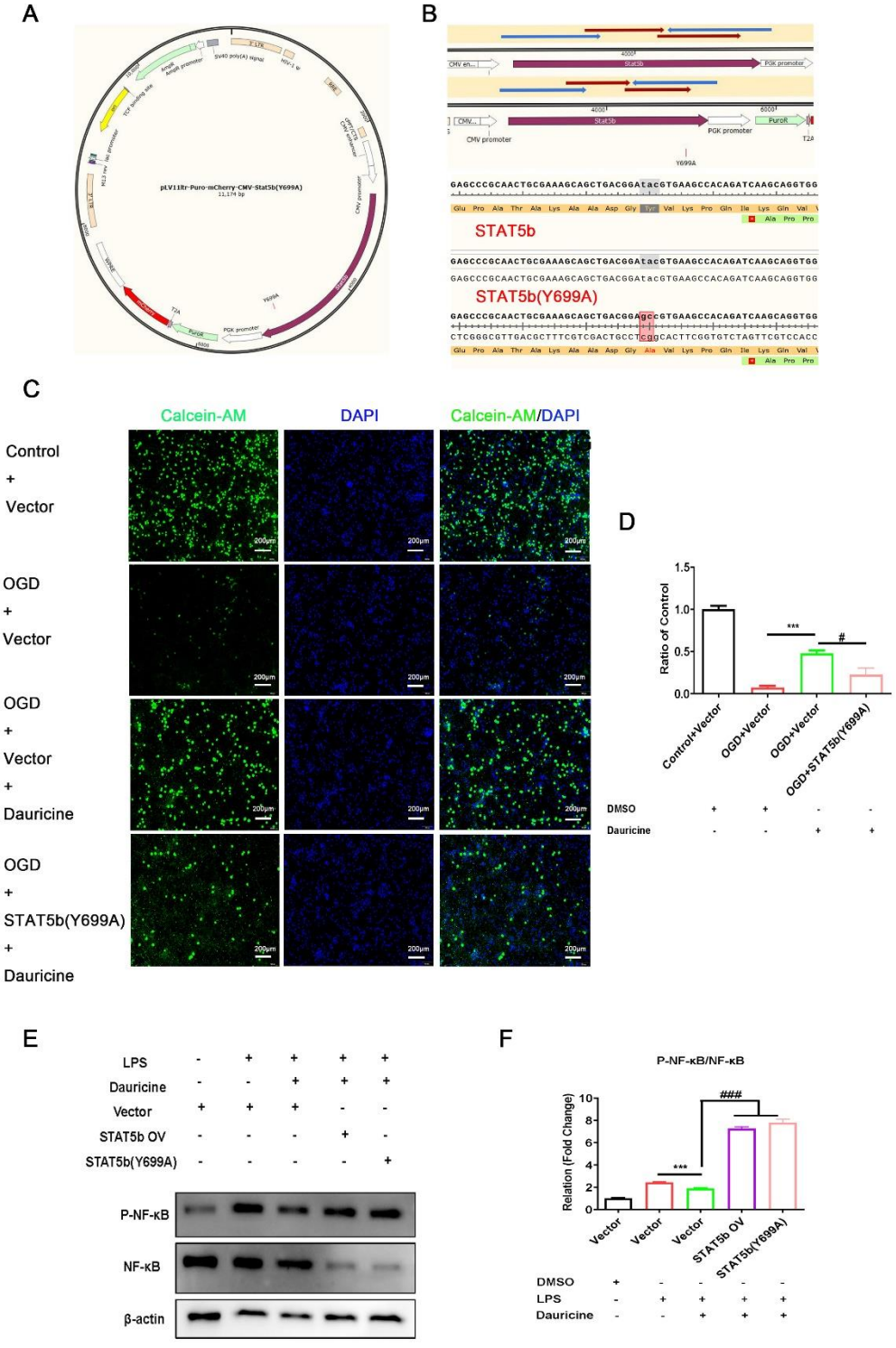

Figure 7. STAT5b (Tyr699 mutant) reversed the neuroprotection of neuron and activated the NF-κB pathway of microglia. (A) Vector map of STAT5b (Tyr-699 mutation). (B) Sequencing and

 doi:10.20944/preprints202208.0158.v1

matching results of STAT5b OV and STAT5b (Y699A). (D) The primary neurons were transfected with STAT5b OV and STAT5b (Y699A) plasmids for 48h, and the neurons were deprived of oxygen and sugar for 30 mins, then reperfusion for 3h, and neurons were stained with calcein-AM and DAPI. n=5, (OGD+Vector) group vs (OGD+Vector +dauricine) group, ***P < 0.001; (OGD+Vector +dauricine) group vs (OGD+STAT5b (Y699A) +dauricine) group, #P < 0.05, unpaired Student's t test. (E) STAT5b OV and STAT5b (Y699A) plasmids were transfected into primary microglia for 48h, and induced by LPS or LPS+dauricine for 3 h, then dected by the western blot and representative figure of NF-κB, P-NF-κB, and β-actin were shown, and was counted with ratio of P-NF-κB to NF-κB (F). n=3, (Vector+LPS) group vs (Vector+LPS+Dauricine) group, ***P < 0.001; (Vector+LPS+Dauricine) group vs (STAT5b OV+LPS+Dauricine) group or (STAT5b (Y699A) + LPS+Dauricine) group, ###p < 0.001, unpaired Student's t test.

We also detected the effect of STAT5b (Y699A) on the NF-κB pathway, and found STAT5b (Y699A) reversed the suppression of dauricine on P-NF-κB of microglia (**Figure 7E-7F)**. These results suggested that dauricine might bind to Tyr-699 phosphorylation region of STAT5b to suppress the activation of NF-κB pathway.

4. Discussion

Plaque inflammation contributes to stroke, and identification of recurrent stroke is improved by the risk score of carotid plaque inflammation(Kelly et al., 2020). Inflammatory cascade starts in hypoperfused vessels and the ischemic brain parenchyma, and inflammatory mediators generates the systemic immune response(Anrather and Iadecola, 2016). In the acute phage of ischemic stroke, first activates microglia, and releases large of inflammation and chemokines, then other immune cells are invaded to the peri-infarct and infarct core, and final the inflammatory response is aggravated by the resident and infiltrating immune cells orchestrate together, including cytokine(Lambertsen et al., 2019). The dynamic balance between pro- and anti-inflammatory responses can be better understood as a basis for designing effective therapies(Jin et al., 2013). We focused on the mechanism of inflammation and stroke, and found that the new inhibitor of STAT5 has well anti-inflammation effect and neuroprotection in the vivo and vitro of experimental models of stroke. Dauricine might be first time to be recognized as inhibitor of STAT5 in this study, and it exhibited powerful anti-inflammatory in the inflammation storm induced by LPS in the primary microglia and reduced the brain injury in the MCAO-reperfusion mouse model.

STAT5 and related signaling pathway play crucial role in autoimmunity and neuroinflammation(Kadekar et al., 2020; Monaghan et al., 2021). STAT5 deficiency induced γδT17 cells lacking and displayed a profound resistance to experimental autoimmune encephalomyelitis, and γδT17 cell expansion is promoted and gut-associated T-bet downregulated mainly by STAT5a homolog rather than STAT5b(Kadekar et al., 2020). STAT5 tetramers promote the pathogenesis of experimental autoimmune encephalomyelitis, and production of CCL17 is regulated by GM-CSF-mediated STAT5 tetramerization through monocyte-derived cells in the STAT5 tetramer-deficient - N-domain double knockin mouse(Monaghan et al., 2021). Th17 cells is converted into cells that mediate IL-9-dependent effects by STAT5 and BATF in allergic airway inflammation and anti-tumor immunity(Fu et al., 2020). The threshold of STAT3, STAT5a, and STAT5b expression determines if PRR-induced proinflammatory cytokines are increased or decreased(Hedl et al., 2019). STAT5 inhibitor substantially decreased inflammation in cardiac hypertrophy in Ang II-induced mice(Jin et al., 2022), and STAT5 inhibitor significantly attenuated atherosclerosis via decreasing inflammation in ApoE-/- mice induced by HFD(Wang et al., 2021). Therefore, STAT5 is an important therapeutic target in anti-inflammation, and the inhibitor has great pharmacological value. In our study, we found an new inhibitor of STAT5 that is dauricine, which regulated the function of microglia and plays a powerful anti-inflammation role, and protested the brain against neuroinflammation post-MCAO reperfusion. AutoDock and PyMOL analyzed that dauricine bind with STAT5b at phosphorylated region Tyr-699 stronger than STAT5a.

 doi:10.20944/preprints202208.0158.v1

NF-κB plays a vital role in the expression of proinflammatory genes including cytokines, chemokines, and adhesion molecules, therefore is well known to be considered as proinflammatory signaling pathway, and is also considered as a target for new anti-inflammatory drugs, called the "holy grail" (Lawrence, 2009). NF-κB is involved in acute inflammation induced by LPS(Lai et al., 2017) and carrageenan(El-Shitany and Eid, 2019), and chronic inflammation including type 2 diabetes(Davari et al., 2020), oral mucosa inflammation(Li and Li, 2020), environment-derived osteoarthritis(Buhrmann et al., 2021), and so on. STAT5 and NF-κB was assessed statistically higher in peripheral blood leukocytes of patients with axSpA(Swierkot et al., 2015). Suppression of NF-κB can mediate through the JAK2-STAT5 pathway(Lan et al., 2020). Therefore, we hypothesized that dauricine reduced the neuroinflammation of post-MCAO reperfusion via mediating the NF-κB activation by inhibiting the STAT5.

It has been benefit for secondary prevention with anti-inflammatory agents in coronary disease(Kelly et al., 2021). STAT5b activation represents a novel therapeutic target, and STAT5b maintains colonic barrier integrity by modulating NF-κB activation in inflammatory bowel disease(Han et al., 2009). In focal cerebral ischaemia and reperfusion rats, STAT5b was confirmed to be significantly modulated in the hippocampus(Sun et al., 2007). However, the research of STAT5b on brain injury caused by focal cerebral ischaemia and reperfusion has not yet been well recognised, and whether the relation to neuroinflammation also has not been well studied. In our study, we focused on stroke with neuroinflammation, and revealed the effect of STAT5 on stroke through anti-inflammation, shown as **Figure 8**. Dauricine was first to be suggested as a new inhibitor of STAT5, and exhibited the potential therapeutic target of STAT5b inhibitor on neuroinflammation of brain injury of MCAO-reperfusion, but more evidence, such as STAT5b know-out mouse, is needed to clarify this hypothesis in the future works.

Preprints (www.preprints.org) | NOT PEER-REVIEWED | Posted: 8 August 2022 doi:10.20944/preprints202208.0158.v1

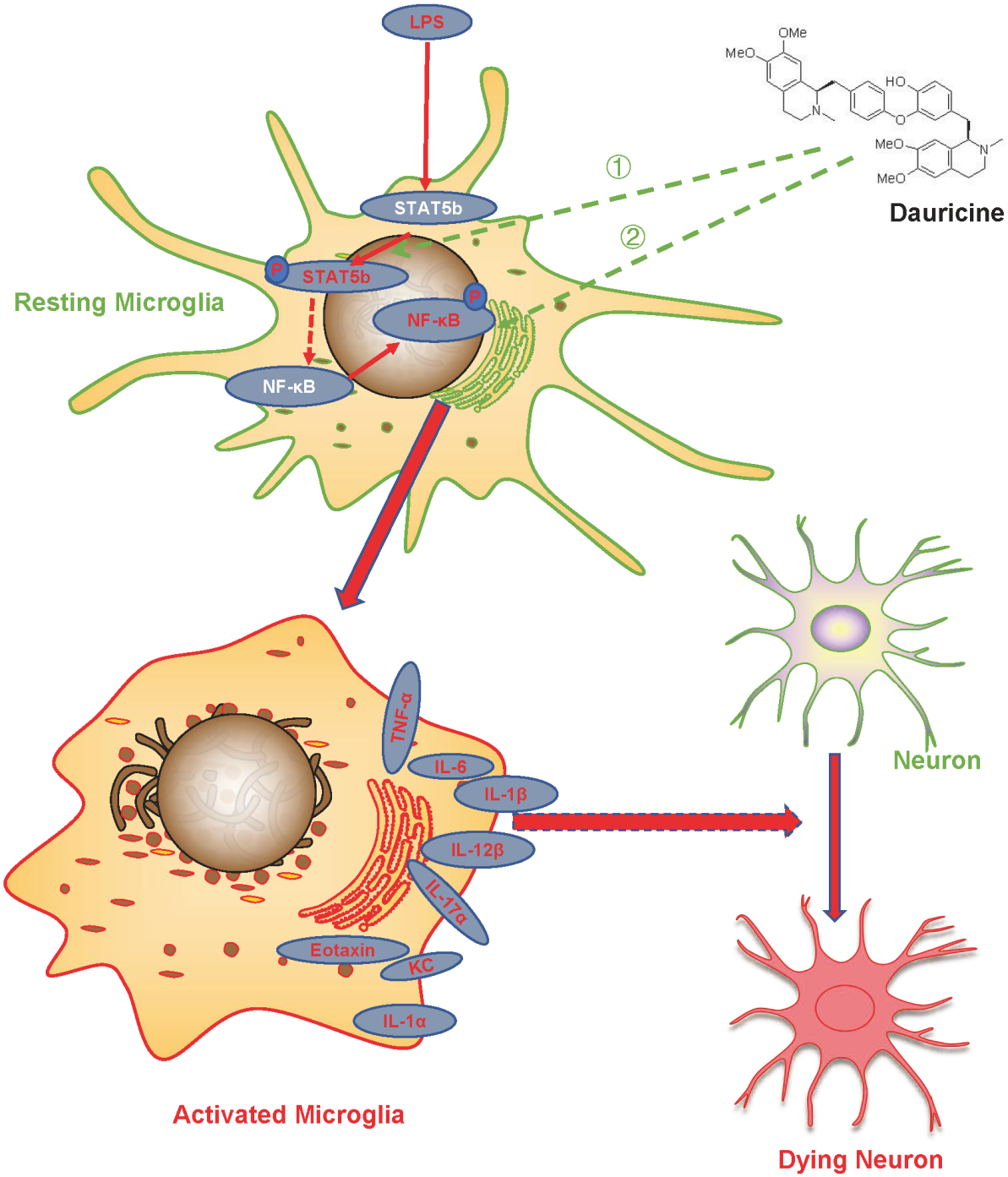

Figure 8. Schematic diagram of the mechanisms underlying the role of dauricine on regulating the microglia activation and protecting neurons from ischemia-reperfusion injury.

5. Conclusion

Dauricine suppressed the inflammation storm and protected the brain from the injury of post-ischemia-reperfusion. It is the first time to find that dauricine regulates the microglia activation and protects neurons from ischemia-reperfusion injury could through inhibiting the STAT5- NF-κB pathway. Those founds revealed that the anti-inflammation and neuroprotection mechanism of dauricine might suppress microglia activation via targeting inhibition of STAT5-NF-κB in the ischemic *stroke*.

 doi:10.20944/preprints202208.0158.v1

Ethics approval: Manuscripts reporting studies not involved human participants, human data or human tissue. The experimental animal ethics review protocol for Drum Tower Hospital at Nanjing University has been approved, the Experimental Animal Ethics Committee has examined the protocol, and the studies were conducted according to the guidelines set by Nanjing University's Guide for Animal Care and Use Committee.

Consent for publication: Not applicable. This manuscript does not contain any individual person`s data.

Availability of data and materials: Data sharing not applicable to this article as no datasets were generated or analysed during the current study.

Funding: This work was supported by the Key Research and Development Program of Jiangsu Province of China (BE2020620), Jiangsu Province Key Medical Discipline (ZDXKA2016020) and the National Natural Science Foundation of China (81920108017, 82130036, 81630028).

Competing interests: The authors declare that they have no competing interests.

Authors' contributions: Zhijun Pu performed the main experiment and wrote the manuscript; Shengnan Xia and Pengfei Shao generated the tMCAO mouse models; Xinyu Bao was responsible for the primary microglial cell culture; Dan Wu analyzed the data and revised the manuscript; Yun Xu provided valuable comments and revised the manuscript. All authors read and approved the final version of the manuscript.

Acknowledgements: Not applicable. Only the authors listed on the manuscript contributed towards the article and they are all listed in the author list.

References

Alamri, F.F., Shoyaib, A.A., Biggers, A., Jayaraman, S., Guindon, J., and Karamyan, V.T. (2018). Applicability of the grip strength and automated von Frey tactile sensitivity tests in the mouse photothrombotic model of stroke. Behav Brain Res *336*, 250-255.

Anrather, J., and Iadecola, C. (2016). Inflammation and Stroke: An Overview. Neurotherapeutics *13*, 661-670.

Buhrmann, C., Brockmueller, A., Mueller, A.L., Shayan, P., and Shakibaei, M. (2021). Curcumin Attenuates Environment-Derived Osteoarthritis by Sox9/NF-kB Signaling Axis. Int J Mol Sci *22*.

Cen, J., Liu, L., Li, M.S., He, L., Wang, L.J., Liu, Y.Q., Liu, M., and Ji, B.S. (2013). Alteration in P-glycoprotein at the blood-brain barrier in the early period of MCAO in rats. J Pharm Pharmacol *65*, 665-672.

Chen, J., Sanberg, P.R., Li, Y., Wang, L., Lu, M., Willing, A.E., Sanchez-Ramos, J., and Chopp, M. (2001). Intravenous administration of human umbilical cord blood reduces behavioral deficits after stroke in rats. Stroke *32*, 2682-2688.

Davari, M., Hashemi, R., Mirmiran, P., Hedayati, M., Sahranavard, S., Bahreini, S., Tavakoly, R., and Talaei, B. (2020). Effects of cinnamon supplementation on expression of systemic inflammation factors, NF-kB and Sirtuin-1 (SIRT1) in type 2 diabetes: a randomized, double blind, and controlled clinical trial. Nutr J *19*, 1.

Egashira, Y., Suzuki, Y., Azuma, Y., Takagi, T., Mishiro, K., Sugitani, S., Tsuruma, K., Shimazawa, M., Yoshimura, S., Kashimata, M., *et al.* (2013). The growth factor progranulin attenuates neuronal injury induced by cerebral ischemia-reperfusion through the suppression of neutrophil recruitment. J Neuroinflammation *10*, 105.

El-Shitany, N.A., and Eid, B.G. (2019). Icariin modulates carrageenan-induced acute inflammation through HO-1/Nrf2 and NF-kB signaling pathways. Biomed Pharmacother *120*, 109567.

Fu, Y., Wang, J., Panangipalli, G., Ulrich, B.J., Koh, B., Xu, C., Kharwadkar, R., Chu, X., Wang, Y., Gao, H., *et al.* (2020). STAT5 promotes

 doi:10.20944/preprints202208.0158.v1

accessibility and is required for BATF-mediated plasticity at the Il9 locus. Nat Commun *11*, 4882.

Goshi, N., Morgan, R.K., Lein, P.J., and Seker, E. (2020). A primary neural cell culture model to study neuron, astrocyte, and microglia interactions in neuroinflammation. J Neuroinflammation *17*, 155.

Guo, S., Tjarnlund-Wolf, A., Deng, W., Tejima-Mandeville, E., Lo, L.J., Xing, C., Arai, K., Ning, M., Zhou, Y., and Lo, E.H. (2018). Comparative transcriptome of neurons after oxygen-glucose deprivation: Potential differences in neuroprotection versus reperfusion. J Cereb Blood Flow Metab *38*, 2236-2250.

Han, X., Ren, X., Jurickova, I., Groschwitz, K., Pasternak, B.A., Xu, H., Wilson, T.A., Hogan, S.P., and Denson, L.A. (2009). Regulation of intestinal barrier function by signal transducer and activator of transcription 5b. Gut *58*, 49-58.

Hedl, M., Sun, R., Huang, C., and Abraham, C. (2019). STAT3 and STAT5 Signaling Thresholds Determine Distinct Regulation for Innate Receptor-Induced Inflammatory Cytokines, and STAT3/STAT5 Disease Variants Modulate These Outcomes. J Immunol *203*, 3325-3338.

Hou, D., Wang, C., Ye, X., Zhong, P., and Wu, D. (2021). Persistent inflammation worsens short-term outcomes in massive stroke patients. BMC Neurol *21*, 62.

Hu, J., Chen, R., An, J., Wang, Y., Liang, M., and Huang, K. (2021). Dauricine Attenuates Vascular Endothelial Inflammation Through Inhibiting NF-kappaB Pathway. Front Pharmacol *12*, 758962.

Jin, G., Wang, L., and Ma, J. (2022). Inhibiting STAT5 significantly attenuated Ang II-induced cardiac dysfunction and inflammation. Eur J Pharmacol *915*, 174689.

Jin, R., Liu, L., Zhang, S., Nanda, A., and Li, G. (2013). Role of inflammation and its mediators in acute ischemic stroke. J Cardiovasc Transl Res *6*, 834-851.

Kadekar, D., Agerholm, R., Rizk, J., Neubauer, H.A., Suske, T., Maurer, B., Vinals, M.T., Comelli, E.M., Taibi, A., Moriggl, R., *et al.* (2020). The neonatal microenvironment programs innate gammadelta T cells through the transcription factor STAT5. J Clin Invest *130*, 2496-2508.

Kelly, P.J., Camps-Renom, P., Giannotti, N., Marti-Fabregas, J., McNulty, J.P., Baron, J.C., Barry, M., Coutts, S.B., Cronin, S., Delgado-Mederos, R., *et al.* (2020). A Risk Score Including Carotid Plaque Inflammation and Stenosis Severity Improves Identification of Recurrent Stroke. Stroke *51*, 838-845.

Kelly, P.J., Camps-Renom, P., Giannotti, N., Marti-Fabregas, J., Murphy, S., McNulty, J., Barry, M., Barry, P., Calvet, D., Coutts, S.B., *et al.* (2019). Carotid Plaque Inflammation Imaged by (18)F-Fluorodeoxyglucose Positron Emission Tomography and Risk of Early Recurrent Stroke. Stroke *50*, 1766-1773.

Kelly, P.J., Lemmens, R., and Tsivgoulis, G. (2021). Inflammation and Stroke Risk: A New Target for Prevention. Stroke *52*, 2697-2706.

Lai, J.L., Liu, Y.H., Liu, C., Qi, M.P., Liu, R.N., Zhu, X.F., Zhou, Q.G., Chen, Y.Y., Guo, A.Z., and Hu, C.M. (2017). Indirubin Inhibits LPS-Induced Inflammation via TLR4 Abrogation Mediated by the NF-kB and MAPK Signaling Pathways. Inflammation *40*, 1-12.

Lambertsen, K.L., Finsen, B., and Clausen, B.H. (2019). Post-stroke inflammation-target or tool for therapy? Acta Neuropathol *137*, 693-714.

Lan, W., Wang, Z., Liu, J., and Liu, H. (2020). Methionyl-Methionine Exerts Anti-Inflammatory Effects through the JAK2-STAT5-NF-kappaB and MAPK Signaling Pathways in Bovine Mammary Epithelial Cells. J Agric Food Chem *68*, 13742-13750.

Lawrence, T. (2009). The nuclear factor NF-kappaB pathway in inflammation. Cold Spring Harb Perspect Biol *1*, a001651.

Li, H., Chen, X., and Zhou, S.J. (2018). Dauricine combined with clindamycin inhibits severe pneumonia co-infected by influenza virus H5N1 and Streptococcus pneumoniae in vitro and in vivo through NF-kappaB signaling pathway. J Pharmacol Sci *137*, 12-19.

Li, M., and Li, R. (2020). IL-2 regulates oral mucosa inflammation through inducing endoplasmic reticulum stress and activating the NF-kB pathway. J Recept Signal Transduct Res *40*, 187-193.

Li, Y.H., and Gong, P.L. (2007). Neuroprotective effects of dauricine against apoptosis induced by transient focal cerebral ischaemia in rats via a mitochondrial pathway. Clin Exp Pharmacol Physiol *34*, 177-184.

Ma, Y., Wang, J., Wang, Y., and Yang, G.Y. (2017). The biphasic function of microglia in ischemic stroke. Prog Neurobiol *157*, 247-272.

 doi:10.20944/preprints202208.0158.v1

Meng, H., Fan, L., Zhang, C.J., Zhu, L., Liu, P., Chen, J., Bao, X., Pu, Z., Zhu, M.S., and Xu, Y. (2021). Synthetic VSMCs induce BBB disruption mediated by MYPT1 in ischemic stroke. iScience *24*, 103047.

Meng, H., Zhao, H., Cao, X., Hao, J., Zhang, H., Liu, Y., Zhu, M.S., Fan, L., Weng, L., Qian, L., *et al.* (2019). Double-negative T cells remarkably promote neuroinflammation after ischemic stroke. Proc Natl Acad Sci U S A *116*, 5558-5563.

Monaghan, K.L., Aesoph, D., Ammer, A.G., Zheng, W., Rahimpour, S., Farris, B.Y., Spinner, C.A., Li, P., Lin, J.X., Yu, Z.X., *et al.* (2021). Tetramerization of STAT5 promotes autoimmune-mediated neuroinflammation. Proc Natl Acad Sci U S A *118*.

Peng, C., Fu, X., Wang, K., Chen, L., Luo, B., Huang, N., Luo, Y., and Chen, W. (2022). Dauricine alleviated secondary brain injury after intracerebral hemorrhage by upregulating GPX4 expression and inhibiting ferroptosis of nerve cells. Eur J Pharmacol *914*, 174461.

Qiao, B., Wang, H., Wang, C., Liang, M., Huang, K., and Li, Y. (2019). Dauricine negatively regulates lipopolysaccharide- or cecal ligation and puncture-induced inflammatory response via NF-kappaB inactivation. Arch Biochem Biophys *666*, 99-106.

Seeliger, D., and de Groot, B.L. (2010). Ligand docking and binding site analysis with PyMOL and Autodock/Vina. J Comput Aided Mol Des *24*, 417-422.

Sun, S.L., Li, T.J., Yang, P.Y., Qiu, Y., and Rui, Y.C. (2007). Modulation of signal transducers and activators of transcription (STAT) factor pathways during focal cerebral ischaemia: a gene expression array study in rat hippocampus after middle cerebral artery occlusion. Clin Exp Pharmacol Physiol *34*, 1097-1101.

Swierkot, J., Sokolik, R., Czarny, A., Zaczynska, E., Nowak, B., Chlebicki, A., Korman, L., Madej, M., Wojtala, P., Lubinski, L., *et al.* (2015). Activity of JAK/STAT and NF-kB in patients with axial spondyloarthritis. Postepy Hig Med Dosw (Online) *69*, 1291-1298.

Wang, X., Ding, X., Yan, J., Lu, Z., Cao, H., Ni, X., and Ying, Y. (2021). STAT5 inhibitor attenuates atherosclerosis via inhibition of inflammation: the role of STAT5 in atherosclerosis. Am J Transl Res *13*, 1422-1431.

Wei, G., Jiang, D., Hu, S., Yang, Z., Zhang, Z., Li, W., Cai, W., and Liu, D. (2021). Polydopamine-Decorated Microcomposites Promote Functional Recovery of an Injured Spinal Cord by Inhibiting Neuroinflammation. ACS Appl Mater Interfaces *13*, 47341-47353.

Wu, N., Zhang, X., Bao, Y., Yu, H., Jia, D., and Ma, C. (2019). Down-regulation of GAS5 ameliorates myocardial ischaemia/reperfusion injury via the miR-335/ROCK1/AKT/GSK-3beta axis. J Cell Mol Med *23*, 8420-8431.

Yang, X.Y., Jiang, S.Q., Zhang, L., Liu, Q.N., and Gong, P.L. (2007). Inhibitory effect of dauricine on inflammatory process following focal cerebral ischemia/reperfusion in rats. Am J Chin Med *35*, 477-486.

Yang, X.Y., Liu, Q.N., Zhang, L., Jiang, S.Q., and Gong, P.L. (2010). Neuroprotective effect of dauricine after transient middle cerebral artery occlusion in rats: involvement of Bcl-2 family proteins. Am J Chin Med *38*, 307-318.

Zhang, F., Yan, C., Wei, C., Yao, Y., Ma, X., Gong, Z., Liu, S., Zang, D., Chen, J., Shi, F.D., *et al.* (2018). Vinpocetine Inhibits NF-kappaB-Dependent Inflammation in Acute Ischemic Stroke Patients. Transl Stroke Res *9*, 174-184.

Zhang, M.J., Sun, J.J., Qian, L., Liu, Z., Zhang, Z., Cao, W., Li, W., and Xu, Y. (2011). Human umbilical mesenchymal stem cells enhance the expression of neurotrophic factors and protect ataxic mice. Brain Res *1402*, 122-131.

Zhang, Z., Cao, X., Bao, X., Zhang, Y., Xu, Y., and Sha, D. (2020). Cocaine- and amphetamine-regulated transcript protects synaptic structures in neurons after ischemic cerebral injury. Neuropeptides *81*, 102023.

Zhao, J., Lian, Y., Lu, C., Jing, L., Yuan, H., and Peng, S. (2012). Inhibitory effects of a bisbenzylisoquinline alkaloid dauricine on HERG potassium channels. J Ethnopharmacol *141*, 685-691.